

# Characterization of Spherical Microlatex Particles Made of Linear Uncrosslinked Polystyrene Chains

JUN GAO, SHUIQIN ZHOU, and CHI WU\*

Department of Chemistry  
The Chinese University of Hong Kong  
Shatin, N.T., Hong Kong

Laser light scattering (LLS), including both angular dependence of the absolute scattering intensity (static LLS) and of the line-width distribution  $G(\Gamma)$  (dynamic LLS), were used to characterize two kinds of pauci-chain polystyrene (PCPS) microlatexes (latex-1 and latex-2). Each PCPS particle contains only a few linear uncrosslinked polystyrene chains. In static LLS, the weight-average particle molar mass ( $M_w$ ) was measured; and simultaneously in dynamic LLS, the diffusion coefficient distribution was obtained from Laplace inversion of precisely measured intensity-intensity time correlation function. Our results reveal that, on average, latex-1 and latex-2 contain  $\sim 13$  and  $\sim 7$  linear polystyrene chains, resp. A combination of both static and dynamic LLS results enables us to calculate the average density of PCPS. Our results have also shown that the particle density of latex-1 and latex-2 are 0.90 and 0.80 g/cm<sup>3</sup>, respectively, which are lower than the density of conventional polystyrene latex particles or bulk polystyrene. Our results imply that the particle density decreases as the average number of polystyrene chains inside the particles decreases.

## INTRODUCTION

Microemulsion polymerization started about 20 years ago (1). Since then, it has become a rapidly developing research field. It is known that narrowly distributed spherical polystyrene (PS) microlatex particles can be made by microemulsion polymerization. These polystyrene latex particles have been extensively used in research and industrial applications. Usually, a conventional PS latex particle contains many crosslinked polymer chains. Recently, Guo *et al.* (2) showed that it was possible to prepare pauci-chain polystyrene (PCPS) microlatex particles by a free radical polymerization of styrene in microemulsion without adding crosslinking agent, namely, each particle contains only a few linear uncrosslinked polystyrene chains. Unlike conventional polystyrene latex particles or bulk polystyrene in which a polymer chain occupies only a few percent of its total accessible space, as predicted by Flory for a random coil chain (3), the polymer chains inside a small PCPS microlatex particle are much confined in space. Therefore, PCPS has a higher density. However, Qian *et al.* (4) have predicted that PCPS has a lower density in comparison with conventional polystyrene latex particles or bulk polystyrene (1.05 g/cm<sup>3</sup>) on the basis of chain

rigidity. This prediction has been confirmed by Wu *et al.* (5).

The next question is when a PCPS particle will lose this unique lower density as the number of polystyrene chains inside a PCPS particle increases. To answer this question, we have to establish a reliable method to determine on average how many chains each PCPS particle contains and the density of the PCPS particles. In the following, we will demonstrate a recently established laser light scattering (LLS) method by using two different kinds of PCPS microlatex particles.

## LASER LIGHT SCATTERING (LLS)

In static LLS, the angular dependence of the excess absolute time-averaged scattering intensity, known as the excess Rayleigh ratio [ $R_{v0}(\theta)$ ], was measured. For a dilute solution at the concentration  $C$  (g/mL) and the scattering angle  $\theta$ ,  $R_{v0}(\theta)$  can be approximately expressed as (6):

$$\frac{KC}{R_{v0}(\theta)} \cong \frac{1}{M_w} \left( 1 + \frac{1}{3} \langle R_g^2 \rangle q^2 \right) + 2A_2C \quad (1)$$

where  $K = 4\pi^2 n_s^2 (dn/dc)^2 / (N_A \lambda_0^4)$  and  $q = 4\pi n_s / \lambda_0 \sin(\theta/2)$  with  $N_A$ ,  $dn/dc$ ,  $n_s$ , and  $\lambda_0$  being Avogadro's constant, the specific refractive index increment, the solvent refractive index and the wavelength of light in vacuo, respectively.  $M_w$  is the weight-average molar

\* To whom correspondence should be addressed.

mass;  $A_2$ , the second virial coefficient; and  $(R_g^2)_z^{1/2}$ , or written as  $\bar{R}_g$ , the z-average root-mean-square radius of gyration. By measuring  $R_{vv}(\theta)$  at a set of  $C$  and  $\theta$ , we can determine  $M_w$ ,  $\bar{R}_g$  and  $A_2$  from  $[KC/R_{vv}(\theta)]_{q \rightarrow 0, c \rightarrow 0}$ ,  $[KC/R_{vv}(\theta)]_{c \rightarrow 0}$ , vs.  $q^2$ , and  $[KC/R_{vv}(\theta)]_{q \rightarrow 0}$  vs.  $C$ .

In dynamic LLS, an intensity-intensity time correlation function  $G^{(2)}(t, \theta)$  in the self-beating mode was measured, which has the form of (7, 8).

$$G^{(2)}(t, \theta) = \langle I(t, \theta)I(0, \theta) \rangle = A[1 + \beta|g^{(1)}(t, \theta)|^2] \quad (2)$$

where  $A$  is a measured baseline;  $\beta$ , a parameter depending on the coherence of the detection;  $t$ , the delay time; and  $g^{(1)}(t, \theta)$ , the normalized first-order electric field time correlation function. For a polydisperse sample,  $g^{(1)}(t, \theta)$  is related to the line-width distribution  $G(\Gamma)$  by

$$g^{(1)}(t, \theta) = \langle E(t, \theta)E^*(0, \theta) \rangle = \int_0^\infty G(\Gamma)e^{-\Gamma t} d\Gamma \quad (3)$$

The widely accepted Laplace inversion program CONTIN (9) was used to calculate  $G(\Gamma)$  from  $G^{(2)}(t, \theta)$ . Normally,  $\Gamma$  is a function of both  $C$  and  $\theta$  (10). At  $C \rightarrow 0$  and  $\theta \rightarrow 0$ ,  $\Gamma$  is related to the translational diffusion coefficient  $D$  by  $\Gamma/q^2 = D$ .  $D$  can be further related to the hydrodynamic radius  $R_h$  by the Stokes-Einstein equation,  $R_h = k_B T / (6\pi\eta D)$  with  $k_B$ ,  $T$  and  $\eta$  being the Boltzmann constant, the absolute temperature and the solvent viscosity, resp.

## EXPERIMENTAL

### Sample Preparation

Two kinds of PCPS microlatex particles, denoted as latex-1 and latex-2 hereafter, were made in the Institute of Chemistry, The Chinese Academy of Sciences, Beijing, China. The compositions of the microemulsion for preparing latex-1 and latex-2 are as follows: (6.00 g styrene plus 0.26 g sodium dodecyl sulfate (SDS)) and (5.00 g styrene plus 0.24 g SDS) respectively in 300 g water. The microemulsion polymerization was carried at 70°C for 20 h with potassium persulfate used as an initiator. After the polymerization, most of the stabilizer (surfactant) molecules were removed by an ion-exchange procedure. The particles are stable in water for a few weeks. Such prepared PCPS particles can be harvested and completely redissolved in THF to form a polystyrene solution. The weight-average molecular weights of the linear polystyrene chains measured by size exclusion chromatography (SEC) for latex-1 and latex-2 are  $1.08 \times 10^6$  and  $7.24 \times 10^5$  g/mol, respectively.

### Instrumentation

A commercial LLS spectrometer (ALV/SP-150, Germany) equipped with an ALV-5000 multi- $\tau$  digital correlator was used with a solid-state laser (ADLAS DPY425II, Germany; output power  $\approx 400$  mW at  $\lambda = 532$  nm) as the light source. The laser beam is verti-

cally polarized. In our present setup, the coherent factor  $\beta$  in dynamic LLS is  $\sim 0.85$ , which is rather high for an LLS spectrometer which is capable of doing both static and dynamic measurement simultaneously. The details of LLS can be found elsewhere (7). It is vital in static LLS to have a precise value of  $dn/dC$ , since the measured  $M_w$  is proportional to  $(dn/dC)^2$ . Recently, a novel differential refractometer was designed and constructed in our laboratory (11), which has been incorporated into our LLS spectrometer, wherein the laser, the thermostat, and the computer are shared. This enables us to measure  $dn/dC$  and the scattered light intensity under identical experimental conditions, so that the wavelength correction is eliminated.

## RESULTS AND DISCUSSION

Figure 1 shows a typical plot of the refractive index increment ( $\Delta n$ ) vs. concentration  $C$  for latex-1. The concentration ranges from  $6.17 \times 10^{-5}$  to  $3.07 \times 10^{-4}$  g/mL and the solvent is deionized water with resistivity of 18.1 M $\Omega \cdot$  cm. The value of  $dn/dC$  determined from the slope of the fitting is  $(0.229 \pm 0.002)$  mL/g at  $T = 25^\circ\text{C}$  and  $\lambda = 532$  nm, which is lower than 0.256 mL/g for conventional polystyrene latex particles (5). This indicates the density of PCPS is lower than conventional polystyrene latex particles or bulk polystyrene since the refractive index is proportional to density.

Figures 2 and 3 respectively show a typical angular and concentration dependence of  $KC/R_{vv}(\theta)$  for latex-1 at  $T = 25^\circ\text{C}$ . For each concentration, the angular extrapolation leads to a corresponding  $[KC/R_{vv}(\theta)]_{\theta \rightarrow 0}$ . The extrapolation of  $[KC/R_{vv}(\theta)]_{\theta \rightarrow 0}$  to infinite dilution leads to  $[KC/R_{vv}(\theta)]_{\theta \rightarrow 0, c \rightarrow 0}$  and further to  $M_w$  on the basis of Eq 1. The values of  $M_w$  of latex-1 and latex-2 are listed in Table 1. It should be noted that the apparent data noise in Figs. 2 and 3 are due to small ordinate scales. Actually, the noise is small. After comparing the particle mass  $M_w$  of latex-1 and latex-2

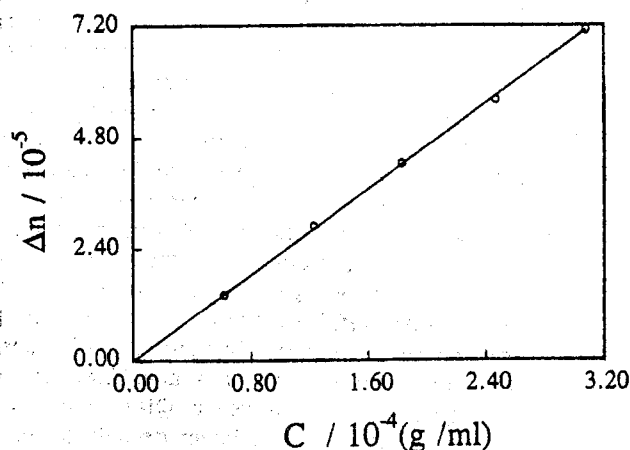


Fig. 1. Typical plot of refractive index increment ( $\Delta n$ ) vs. concentration ( $C$ ) for latex-1 at  $T = 25^\circ\text{C}$  and  $\lambda_0 = 532$  nm. The specific refractive index increment  $dn/dC$  calculated from the least-squares fitting (the line) is 0.229 ml/g.

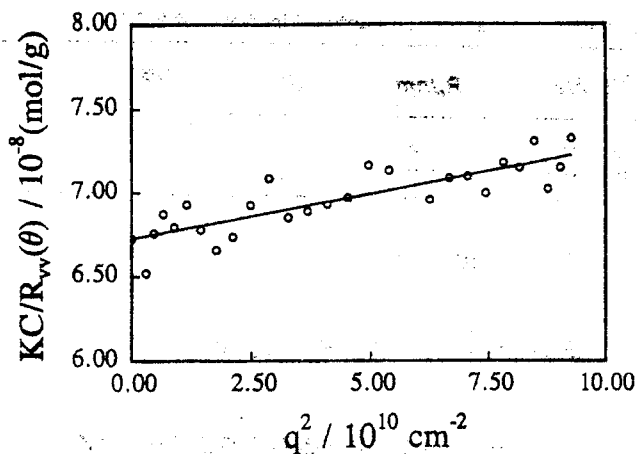


Fig. 2.  $KC/R_w(\theta)$  vs.  $q^2$  for latex-1 at  $C = 1.86 \times 10^{-5}$  g/ml at  $T = 25^\circ\text{C}$ , where  $\theta$  ranges from  $15^\circ$  to  $150^\circ$ .

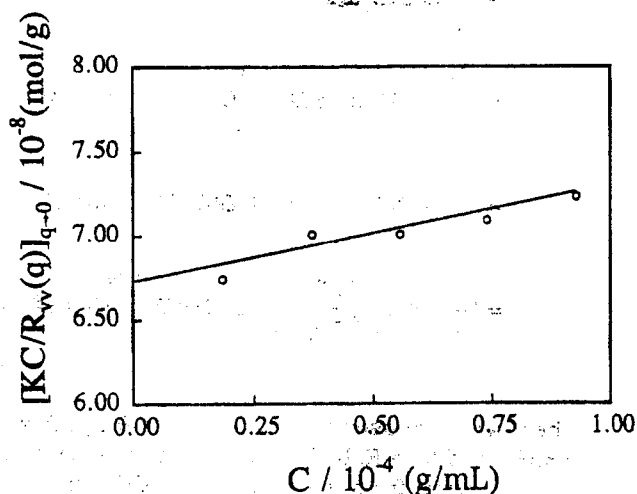


Fig. 3.  $[KC/R_w(q)]_{q=0}$  vs.  $C$  for latex-1 at  $T = 25^\circ\text{C}$ , where  $C$  ranges from  $1.86 \times 10^{-5}$  to  $9.28 \times 10^{-5}$  g/mL.

with previously determined  $M_w$  values of individual linear polystyrene chains, we can calculate that on average each latex-1 and latex-2 particle contains  $\sim 13$  and  $\sim 7$  linear polystyrene chains, respectively.

Figure 4 shows a typical measured intensity-intensity time correlation function for latex-1 at  $C = 9.28 \times 10^{-5}$  g/ml and  $\theta = 20^\circ$ .  $G(\Gamma)$  can be obtained from the Laplace inversion of the measured time correlation function. From  $G(\Gamma)$ , we can calculate the z-average line width  $\bar{\Gamma} = \int_0^\infty G(\Gamma)\Gamma d\Gamma$  and the distribution width  $\mu_2 (= \int_0^\infty G(\Gamma)(\Gamma - \bar{\Gamma})^2 d\Gamma)$ . Experimentally, we found that  $\bar{\Gamma}$  is independent of both  $C$  and  $\theta$ . This is understandable because the particle size is relatively small and the solution is dilute. As mentioned,  $\Gamma$  can be converted to  $D$  or  $R_h$ , so that  $G(\Gamma)$  can be converted into a translational diffusion coefficient distribution  $G(D)$  or a hydrodynamic radius distribution  $f(R_h)$ .

Figure 5 shows a typical translational diffusion coefficient distribution for latex-1 at  $\theta = 20^\circ$  and  $T = 25^\circ\text{C}$ , where  $C = 9.28 \times 10^{-5}$  g/mL. The average values of  $\bar{D} (= \int_0^\infty G(D)D dD)$  and  $\bar{R}_h (= \int_0^\infty f(R_h)R_h dR_h)$  at  $C \rightarrow 0$  and  $\theta \rightarrow 0$  together with the values of the

relative distribution width  $(\mu_2/\bar{D}^2)$  of  $G(D)$  are also listed in Table 1. The ratio of  $\bar{R}_g/\bar{R}_h$  for latex-1 is very close to a theoretical value of  $(3/5)^{1/2}$  for a uniform sphere, which indicates that latex-1 and latex-2 are uniform spherical particles (12).

Using the values of  $M_w$  and  $\bar{R}_h$  listed in Table 1, we can calculate the apparent density of PCPS latex particles by respectively replacing the particle molar mass  $M$  and radius  $R$  with  $M_w$  and  $\bar{R}_h$  in the following definition:

$$M = [(4\pi/3)R^3\rho]N_A \quad (4)$$

Such calculated density values for latex-1 and latex-2 are only  $0.505$  g/cm<sup>3</sup> and  $0.466$  g/cm<sup>3</sup>, much lower than  $1.05$  g/cm<sup>3</sup> for conventional polystyrene latex particles and bulk polystyrene (5), which are unlikely to be true. These are only apparent densities because Eq 4 is valid only for a monodispersed case. Therefore, we have to consider not only the distributions of the particle mass ( $M$ ) and particle size ( $R$ ), but also the fact that  $M_w$  and  $\bar{R}_h$  are different averages by their definitions.

In this study, we have adopted a different way to calculate the particle density ( $\rho$ ), wherein we started with  $G(D)$  instead of  $\bar{D}$ ,  $M$  instead of  $M_w$  and  $R$  instead of  $\bar{R}_h$ . On the one hand, in dynamic LLS, according to the definition of  $|g^{(1)}(t)|$ , when  $t \rightarrow 0$ ,

$$|g^{(1)}(t)|_{t \rightarrow 0} = \langle E(t)E^*(0) \rangle_{t \rightarrow 0} = \int_0^\infty G(\Gamma) d\Gamma \propto \langle I \rangle \quad (5)$$

On the other hand, in static LLS, at  $C \rightarrow 0$  and  $\theta \rightarrow 0$ , the net scattered intensity

$$\langle I \rangle \propto \int_0^\infty f_w(M)M dM \quad (6)$$

where  $f_w(M)$  is a differential molecular weight distribution. A comparison of Eqs 5 and 6 leads to

$$\int_0^\infty G(\Gamma) d\Gamma \propto \int_0^\infty f_w(M)M dM$$

or

$$\int_0^\infty G(D) dD \propto \int_0^\infty f_w(M)M dM \quad (7)$$

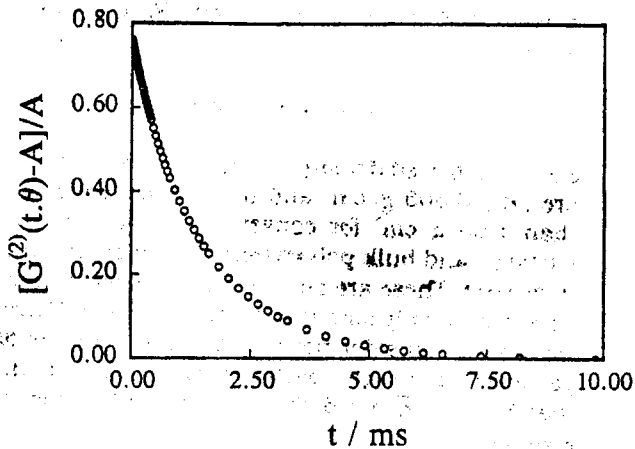
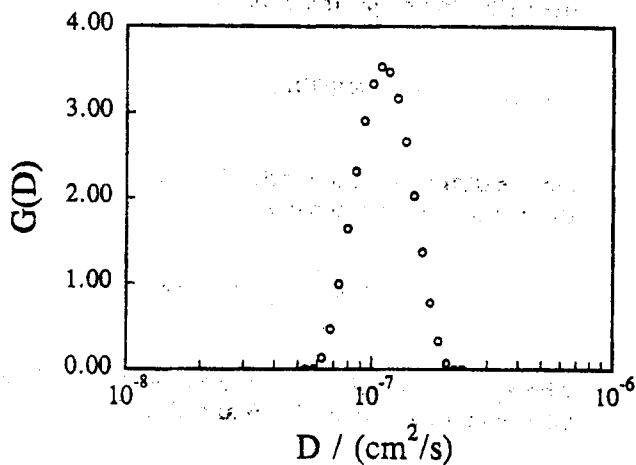
we have used the fact that  $\Gamma = Dq^2$  and  $q$  is a constant for a given  $\lambda$  and  $\theta$ . Equation 7 can also be expressed as

$$\int_0^\infty G(D)D d(\ln D) \propto \int_0^\infty f_w(M)M^2 d(\ln M) \quad (8)$$

where  $d(\ln M) \propto d(\ln R)$  and  $d(\ln R_h) \propto d(\ln D)$  according

Table 1. Summary of Both Static and Dynamic LLS Results of Latex-1 and Latex-2 in Water at 25°C.

Sample	$\frac{dn/dC}{\text{mL/g}}$	$\frac{M_w}{\text{g/mol}}$	$R_p/\text{nm}$	$\bar{D}/\text{cm}^2/\text{s}$	$R_p/\text{nm}$	$\mu_z/\Gamma^2$	$\bar{R}_g/\bar{R}_h$	$\frac{\rho}{\text{g/cm}^3}$
Latex-1	0.229	$1.49 \times 10^7$	15.5	$1.14 \times 10^{-7}$	22.6	0.055	0.7	0.9
Latex-2	0.229	$5.44 \times 10^6$	—	$1.53 \times 10^{-7}$	16.7	0.045	—	0.8


 Fig. 4. Typical measured intensity-intensity time correlation function for latex-1 ( $C = 9.28 \times 10^{-5} \text{ g/mL}$ ) at  $\theta = 20^\circ$  and  $T = 25^\circ\text{C}$ .

 Fig. 5. Typical translational diffusion coefficient distribution for latex-1 at  $c = 9.28 \times 10^{-5} \text{ g/mL}$ ,  $\theta = 20^\circ$  and  $T = 25^\circ\text{C}$ .

to Eq 4 and the Stokes-Einstein equation, respectively, so that Eq 8 can be rewritten as

$$\int_0^\infty G(D)D d(\ln D) \propto \int_0^\infty f_w(M)M^2 d(\ln D) \quad (9)$$

A comparison of the both sides of Eq 9 leads to

$$f_w(M) \propto G(D)D/M^2 \quad (10)$$

Using Eqs 10 and 4, we can calculate the weight-average molar mass of the latex particles according to

the definition of  $M_w$ ,

$$\begin{aligned} (M_w)_{\text{cal}} &= \frac{\int_0^\infty f_w(M)M dM}{\int_0^\infty f_w(M) dM} \\ &= \frac{\int_0^\infty G(D)DM^{-1} dM}{\int_0^\infty G(D)DM^{-2} dM} \\ &= \frac{\int_0^\infty G(D)D d(\ln M)}{\int_0^\infty G(D)DM^{-1} d(\ln M)} \\ &= \frac{\int_0^\infty G(D)D d(\ln D)}{\int_0^\infty G(D)DM^{-1} d(\ln M)} \\ &= \frac{\int_0^\infty G(D)D d(\ln D)}{\int_0^\infty G(D)DM^{-1} d(\ln D)} \\ &= \left(\frac{4}{3}\pi\rho N_A\right) \left(\frac{k_B T}{6\pi\eta}\right)^3 \frac{\int_0^\infty G(D) dD}{\int_0^\infty G(D)D^3 dD} \end{aligned} \quad (11)$$

where we have used that  $M = (4/3)\pi\rho R^3 N_A$ ,  $D = k_B T / (6\pi\eta R_h)$  and  $R_h = R$ . In Eq 11,  $(M_w)_{\text{cal}}$  can be replaced by  $M_w$  measured from static LLS and  $G(D)$  can be obtained from dynamic LLS. Therefore, the only unknown parameter  $\rho$  in Eq 11 can be calculated from a combination of the static and dynamic LLS results. The calculated values of  $\rho$  for latex-1 and latex-2 are 0.71 and 0.68  $\text{g/cm}^3$ , respectively. Such calculated densities of PCPS lattices are still much lower than conventional polystyrene latex particles or bulk polystyrene (known as 1.05  $\text{g/cm}^3$ ). This might be partially attributed to a larger intersegmental distance in PCPS, namely in PCPS the intersegmental crossing occurs mainly within one polymer chain (i.e., the intrachain crossing) because each PCPS particle contains only a few chains. However, in conventional PS latex particles or bulk polystyrene, the interchain crossing will be dominant. Since polymer chains have a certain degree of rigidity, the intrachain crossing should be more difficult in comparison with the interchain crossing, which leads to a larger intersegmental spacing and a lower density. This lower density might also be attributed to the larger apparent hydrodynamic radius, because of the rough surface and trace amounts of surfactant remained on the particle surface. It is known that the surfactant layer thickness ( $b$ ) is  $\sim 50\%$  of the surfactant chain length (13). Therefore,  $R$  should be the difference between  $R_h$  and  $b$ , i.e.,  $R = R_h - b$ . In this way, on the basis of Eq 4 and  $R_h =$

$k_B T / (6\pi\eta D)$ , we have

$$D = \frac{k_B T}{6\pi\eta R_h} = \frac{k_B T}{6\pi\eta} \frac{1}{R+b} = \left( \frac{k_B T}{6\pi\eta} \right) \frac{1}{1+b/R} \frac{1}{R}$$

$$= \frac{(k_B T / 6\pi\eta) ((4/3)\pi\rho N_A)^{1/3}}{1 + b(4\pi\rho N_A / 3M)^{1/3}} M^{-1/3} \quad (12)$$

In Eq 12,  $1 + b(4\pi\rho N_A / 3M)^{1/3}$  can be approximated by  $1 + b(4\pi\rho N_A / 3M_w)^{1/3}$  because  $b \sim 1$  nm which is much smaller than  $R = [3M / (4\pi\rho N_A)]^{1/3}$ . Therefore, Eq 11 should be

$$(M_w)_{cal} = \frac{(k_B T / 6\pi\eta)^3 ((4/3)\pi\rho N_A)}{[1 + b(4\pi\rho N_A / 3M)^{1/3}]^3}$$

$$\int_0^\infty G(D) dD \Big/ \int_0^\infty G(D) D^3 dD \quad (13)$$

There is only one unknown parameter  $\rho$  in Eq 13. We can recalculate  $\rho$  from  $M_w$  and  $G(D)$  obtained from static and dynamic LLS, respectively, on the basis of Eq 13. Such calculated particle densities of latex-1 and latex-2 are 0.90 and 0.80 g/cm<sup>3</sup>, respectively, as listed in Table 1. These values of  $\rho$  are close to previous results on a similar microlatex system (5). It should be noted that  $\rho$  calculated in this way contains  $\sim \pm 5\%$  error.

### CONCLUSIONS

The characterization of two kinds of pauci-chain polystyrene (PCPS) microlatexes (latex-1 and latex-2) has been accomplished by using a combination of static and dynamic laser light scattering results. Our results showed that on average each latex-1 and latex-2 particle contains  $\sim 13$  and  $\sim 7$  linear uncrosslinked polystyrene chains, respectively. Both the specific refractive index increment  $dn/dc$  and the calculated density values are lower than that of conventional polystyrene latex and bulk polystyrene, which suggests that the PCPS microlatex prepared by free radical polymerization of styrene in microemulsions are slightly different with conventional polystyrene latex particles made of crosslinked chains or bulk polystyrene. This density difference might be partially attributed to larger intersegmental distance because the intrachain crossing (or approaching) is more difficult than the interchain crossing.

### ACKNOWLEDGMENT

Thanks are due to Professors R. Qian, X. G. Jin and L. S. Chen (The Institute of Chemistry, Beijing, China) for providing us two PCPS samples. The financial support of the Research Grants Council of Hong Kong

Government Earmarked Grant 1994/95 (CUHK 299/94p, 221600260) is gratefully acknowledged.

### NOMENCLATURE

- LLS = Laser light scattering.  
 PS = Polystyrene.  
 PCPS = Pauci-chain polystyrene.  
 $dn/dc$  = Refractive index increment.  
 $\langle R_g^2 \rangle^{1/2}$  or  $\bar{r}$  = Z-average root-mean-square radius of gyration.  
 $A_2$  = Second-order virial coefficient.  
 $M_w$  = Weight average particle molar mass.  
 $M$  = Particle molar mass.  
 $f_w(M)$  = Weight average molar mass distribution.  
 $\Gamma$  = Line width.  
 $G(\Gamma)$  = Line-width distribution function.  
 $D$  = Translational diffusion coefficient.  
 $G(D)$  = Translational diffusion coefficient distribution function.  
 $\bar{r}$  = z-average root-mean square hydrodynamic radius.  
 $\rho$  = Density.  
 $\beta$  = Coherent factor.  
 $q$  = Scattering vector.  
 $\eta$  = Solvent viscosity.  
 $g^{(1)}(t, \theta)$  = The normalized first-order electric field time correlation function.  
 $G^{(2)}(t, \theta)$  = Intensity-intensity time correlation function.

### REFERENCES

1. S. E. Friberg and P. Bothovel, eds., *Microemulsions: Structure and Dynamics*, CRC, New York (1986).
2. J. S. Guo, M. S. El-Aasser, and J. W. Vanderhoff, *J. Polym. Sci., Polym. Chem. Ed.*, **27**, 691 (1989).
3. P. J. Flory, *Principles of Polymer Chemistry*, Cornell University Press, Ithaca, N.Y. (1953).
4. R. Qian, L. Wu, D. Shen, D. H. Napper, R. A. Mann, and D. F. Sangster, *Macromolecules*, **26**, 2950 (1993).
5. C. Wu, K. K. Chan, K. F. Woo, R. Qian, X. Li, L. Chen, D. H. Napper, G. Tan, and A. J. Hill, *Macromolecules*, **28**, 1592 (1995).
6. B. H. Zimm, *J. Chem. Phys.*, **16**, 1099 (1948).
7. B. Chu, in *Laser Light Scattering*, Academic Press, New York (1974).
8. R. Pecora, in *Dynamic Light Scattering*, Plenum Press, New York (1976).
9. S. W. Provencher, *Biophys. J.*, **16**, 29 (1976); *J. Chem. Phys.*, **64**, 2772 (1976); *Makromol. Chem.*, **180**, 201 (1979).
10. W. H. Stockmayer and M. Schmidt, *Pure. Appl. Chem.*, **54**, 407 (1982); *Macromolecules*, **17**, 509 (1984).
11. C. Wu and K. Q. Xia, *Rev. Sci. Instrum.*, **65**, 587 (1994).
12. G. Gee, *Polymer*, **7**, 177 (1966).
13. C. Wu, *Macromolecules*, **27**, 7099 (1994).